

## Two Metals Are Better than One: Investigations on the Interactions between Dinuclear Metal Complexes and Quadruplex DNA

Kogularamanan Suntharalingam, Andrew J. P. White, and Ramon Vilar\*

*Department of Chemistry, Imperial College London, London SW7 2AZ, U.K.*

Received May 5, 2010

Twelve mono- and dimetallic complexes (the metals being Cu<sup>II</sup>, Pt<sup>II</sup>, and Zn<sup>II</sup>) with terpyridine-based ligands have been prepared and fully characterized. The X-ray crystal structures of two of the complexes (monometallic Cu<sup>II</sup> and Zn<sup>II</sup> complexes with a morpholino-substituted terpyridine ligand) are reported. The affinities of the 12 complexes toward duplex and quadruplex (HTelo and *c-myc*) DNA have been investigated using a combination of techniques including fluorescent indicator displacement (FID) assay, UV–vis spectroscopy and circular dichroism (CD). These studies revealed that the dicopper and diplatinum complexes **11** and **12** bind very strongly to quadruplex DNA (up to  $K = 7.97 \times 10^6 \text{ M}^{-1}$ ) and with good selectivity (up to 100-fold) over duplex DNA. In these dimetallic complexes, one of the metals is coordinated to a terpyridine moiety yielding square based pyramidal (with Cu<sup>II</sup>) or square planar (with Pt<sup>II</sup>) geometries. The second metal is coordinated to a dipicolyl amine linked to terpyridine by a three-atom spacer. We propose that these complexes bind to quadruplex DNA via a combination of interactions:  $\pi$ – $\pi$  end-stacking between the metal-terpyridine fragment and the guanine quartet, and electrostatic/metal-phosphate interactions (between the metal-dipicolyl amine fragment and DNA's backbone).

### Introduction

Guanines have the ability to self-assemble into square structures via hydrogen-bonding. The formation of these tetrads can in turn give rise to quadruply stranded DNA assemblies (known as quadruplexes) which can form inter- or intramolecularly from guanine-rich sequences of DNA.<sup>1–4</sup> Over the past few years, several biological functions have been associated to quadruplexes, making these structures appealing targets for drug development. For example, it has been shown that telomerase (an enzyme overexpressed in approximately 85% of cancer cells which plays an important role in cancer cell immortalization<sup>5,6</sup>) is inhibited if single-stranded telomeric DNA is folded into a quadruplex structure.<sup>7,8</sup> In addition, there is now mounting evidence showing that formation of quadruplexes in guanine-rich regions of the

genome may play important roles in regulating gene expression. For example, the promoter regions of certain oncogenes such as *c-myc* and *c-kit* are guanine rich, and formation of quadruplexes in these regions has been proposed to regulate the corresponding oncogene's transcription.<sup>9–13</sup> Therefore, there is great current interest in developing molecules that induce the formation of quadruplexes in either the telomere or in the promoter regions of oncogenes. Such molecules could provide a basis for the development of novel anticancer drugs.<sup>14</sup> Indeed, several groups have reported molecules which interact strongly with quadruplex DNA and are also able to inhibit telomerase and/or regulate the transcription of certain oncogenes.<sup>15–23</sup>

\*To whom correspondence should be addressed. E-mail: r.vilar@imperial.ac.uk.

(1) Burge, S.; Parkinson, G. N.; Hazel, P.; Todd, A. K.; Neidle, S. *Nucleic Acids Res.* **2006**, *34*, 5402.

(2) Campbell, N. H.; Parkinson, G. N. *Methods* **2007**, *43*, 252.

(3) Neidle, S.; Balasubramanian, S. *Quadruplex Nucleic Acids*; The Royal Society of Chemistry: Cambridge, U.K., 2006.

(4) Neidle, S.; Parkinson, G. N. *Biochimie* **2008**, *90*, 1184.

(5) Kim, N. W.; Piatyszek, M. A.; Prowse, K. R.; Harley, C. B.; West, M. D.; Ho, P. L.; Coviello, G. M.; Wright, W. E.; Weinrich, S. L.; Shay, J. W. *Science* **1994**, *266*, 2011.

(6) Blasco, M. A. *Eur. J. Cell Biol.* **2003**, *82*, 441.

(7) De Cian, A.; Lacroix, L.; Douarre, C.; Temime-Smaali, N.; Trentesaux, C.; Riou, J.-F.; Mergny, J.-L. *Biochimie* **2008**, *90*, 131.

(8) Sun, D.; Thompson, B.; Cathers, B. E.; Salazar, M.; Kerwin, S. M.; Trent, J. O.; Jenkins, T. C.; Neidle, S.; Hurley, L. H. *J. Med. Chem.* **1997**, *40*, 2113.

(9) Rangan, A.; Fedoroff, O. Y.; Hurley, L. H. *J. Biol. Chem.* **2001**, *276*, 4640.

(10) Siddiqui-Jain, A.; Grand, C. L.; Bearss, D. J.; Hurley, L. H. *Proc. Natl. Acad. Sci. U. S. A.* **2002**, *99*, 11593.

(11) Fernando, H.; Reszka, A. P.; Huppert, J.; Ladame, S.; Rankin, S.; Venkitaraman, A. R.; Neidle, S.; Balasubramanian, S. *Biochemistry* **2006**, *45*, 7854.

(12) Rankin, S.; Reszka, A. P.; Huppert, J.; Zloh, M.; Parkinson, G. N.; Todd, A. K.; Ladame, S.; Balasubramanian, S.; Neidle, S. *J. Am. Chem. Soc.* **2005**, *127*, 10584.

(13) Qin, Y.; Hurley, L. H. *Biochimie* **2008**, *90*, 1149.

(14) Balasubramanian, S.; Neidle, S. *Curr. Opin. Chem. Biol.* **2009**, *13*, 345.

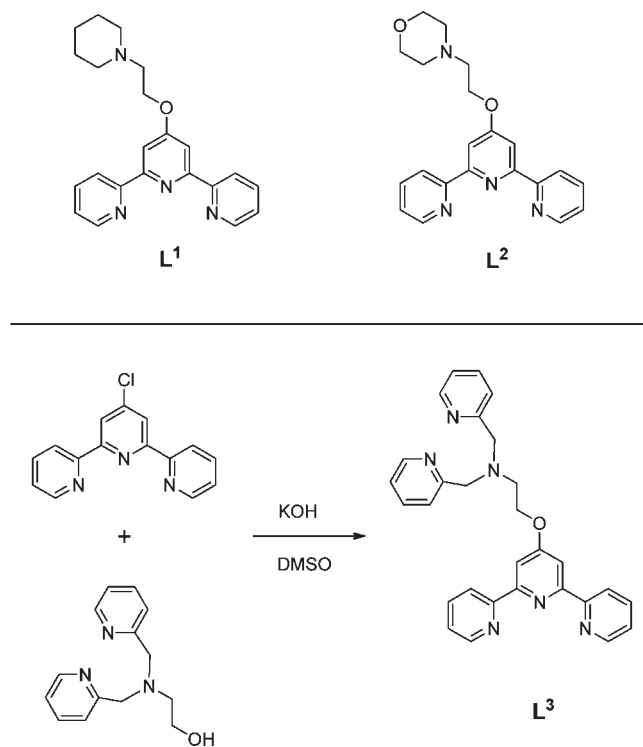
(15) Dash, J.; Shirude, P. S.; Balasubramanian, S. *Chem. Commun.* **2008**, 3055.

(16) Dash, J.; Shirude, P. S.; Hsu, S.-T. D.; Balasubramanian, S. *J. Am. Chem. Soc.* **2008**, *130*, 15950.

(17) Kim, M.-Y.; Gleason-Guzman, M.; Izbicka, E.; Nishioka, D.; Hurley, L. H. *Cancer Res.* **2003**, *63*, 3247.

For quadruplex DNA binders to have real pharmaceutical potential, they should interact strongly with their target and exhibit high selectivity for quadruplex versus duplex DNA. In addition it would be highly desirable to find molecules that are selective for a specific quadruplex structure over others. The prevailing approach when designing quadruplex DNA binders is based on planar molecules<sup>24,25</sup> (either based on organic heteroaromatic systems or, more recently, planar metal complexes<sup>26–34</sup>) possessing the ability to interact via  $\pi$ - $\pi$  stacking with G-quartets. However, it has become evident that other structural features of quadruplexes must also be taken into account when designing binders. For example, quadruplexes contain distinct loops and grooves (the nature of which is sequence- and topology-dependent) and, therefore, interaction of the binder with the phosphate backbone and DNA bases outside of G-tetrads needs to be considered. Indeed, a range of different types of substituents such as amines,<sup>35–37</sup> peptides,<sup>38–40</sup> and amides<sup>41</sup> have been attached to the central  $\pi$ - $\pi$  stacking core of quadruplex binders with the aim of improving their affinity and selectivity toward quadruplex DNA. We rationalized that an alternative approach for the development of more efficient quadruplex DNA binders would be to use metal complexes as

**Scheme 1.** Terpyridine-Based Ligands Used in This Study<sup>a</sup>



<sup>a</sup>**L**<sup>1</sup> and **L**<sup>2</sup> were prepared using the procedure we recently reported. **L**<sup>3</sup> was synthesised as shown in the scheme.

substituents on the  $\pi$ - $\pi$  stacking planar core. This type of substituent would provide the possibility of strong interactions (electrostatic and/or by coordination of the metal center) with the loops and grooves of DNA. Some examples of this approach have been recently reported in which platinum complexes are attached to planar aromatic groups.<sup>31,42,43</sup> In these examples, the planar unit is proposed to interact via  $\pi$ - $\pi$  stacking with the G-quartet, while the tethered platinum coordinates directly to nucleobases present in the loops/grooves of DNA.

In this paper we present a series of terpyridine-based mono- and dimetal complexes (with Cu<sup>II</sup>, Pt<sup>II</sup>, and Zn<sup>II</sup>) as DNA binders (see Schemes 1 and 2). The dinuclear compounds have been designed to interact with the G-quartet via  $\pi$ - $\pi$  stacking (using the square planar/square-based pyramidal metal-terpyridine “core”) and with DNA’s phosphate backbone via direct coordination or electrostatic interactions (using the metal dipicolyl amine motif). To evaluate the effect of these metal-based substituents, the affinity and selectivity of the complexes toward quadruplex and duplex DNA have been investigated.

## Results and Discussion

**Synthesis of **L**<sup>3</sup> and the Corresponding Copper(II), Zinc(II), and Platinum(II) Complexes.** Four different terpyridine ligands were employed in this study (Scheme 1). **L**<sup>1</sup> and **L**<sup>2</sup> were synthesized using the methodology we recently reported<sup>44</sup> while **L**<sup>3</sup>, a new compound, was

(18) Kim, M.-Y.; Vankayalapati, H.; Shin-ya, K.; Wierzba, K.; Hurley, L. H. *J. Am. Chem. Soc.* **2002**, *124*, 2098.

(19) Cheng, M.-K.; Modi, C.; Cookson, J. C.; Hutchinson, I.; Heald, R. A.; McCarrroll, A. J.; Missailidis, S.; Tanious, F.; Wilson, W. D.; Mergny, J.-L.; Laughton, C. A.; Stevens, M. F. G. *J. Med. Chem.* **2008**, *51*, 963.

(20) Hounsou, C.; Guittat, L.; Monchaud, D.; Jourdan, M.; Saettel, N.; Mergny, J.-L.; Teulade-Fichou, M.-P. *ChemMedChem* **2007**, *2*, 655.

(21) Cuenca, F.; Moore, M. J. B.; Johnson, K.; Guyen, B.; De Cian, A.; Neidle, S. *Bioorg. Med. Chem. Lett.* **2009**, *19*, 5109.

(22) Drewe, W. C.; Nanjunda, R.; Gunaratnam, M.; Beltran, M.; Parkinson, G. N.; Reszka, A. P.; Wilson, W. D.; Neidle, S. *J. Med. Chem.* **2008**, *51*, 7751.

(23) Rahman, K. M.; Reszka, A. P.; Gunaratnam, M.; Haider, S. M.; Howard, P. W.; Fox, K. R.; Neidle, S.; Thurston, D. E. *Chem. Commun.* **2009**, 4097.

(24) Arola, A.; Vilar, R. *Curr. Top. Med. Chem.* **2008**, *8*, 1405.

(25) Monchaud, D.; Teulade-Fichou, M.-P. *Org. Biomol. Chem.* **2008**, *6*, 627.

(26) Reed, J. E.; Arnal, A. A.; Neidle, S.; Vilar, R. *J. Am. Chem. Soc.* **2006**, *128*, 5992.

(27) Reed, J. E.; Neidle, S.; Vilar, R. *Chem. Commun.* **2007**, 4366.

(28) Reed, J. E.; White, A. J. P.; Neidle, S.; Vilar, R. *Dalton Trans.* **2009**, 2558.

(29) Arola-Arnal, A.; Benet-Buchholz, J.; Neidle, S.; Vilar, R. *Inorg. Chem.* **2008**, *47*, 11910.

(30) Barry, N. P. E.; Abd Karim, N. H.; Vilar, R.; Therrien, B. *Dalton Trans.* **2009**, 10717.

(31) Bertrand, H.; Bombard, S.; Monchaud, D.; Teulade-Fichou, M.-P. *J. Biol. Inorg. Chem.* **2007**, *12*, 1003.

(32) Bertrand, H.; Monchaud, D.; De Cian, A.; Guillot, R.; Mergny, J.-L.; Teulade-Fichou, M.-P. *Org. Biomol. Chem.* **2007**, *5*, 2555.

(33) Gill, M. R.; Garcia-Lara, J.; Foster, S. J.; Smythe, C.; Battaglia, G.; Thomas, J. A. *Nat. Chem.* **2009**, *1*, 662.

(34) Kieltyka, R.; Englebienne, P.; Fakhoury, J.; Autexier, C.; Moitessier, N.; Sleiman, H. F. *J. Am. Chem. Soc.* **2008**, *130*, 10040.

(35) Bejugam, M.; Sewitz, S.; Shirude, P. S.; Rodriguez, R.; Shahid, R.; Balasubramanian, S. *J. Am. Chem. Soc.* **2007**, *129*, 12926.

(36) Bugaut, A.; Jantos, K.; Wietor, J.-L.; Rodriguez, R.; Sanders, J. K. M.; Balasubramanian, S. *Angew. Chem., Int. Ed.* **2008**, *47*, 2677.

(37) Waller, Z. A. E.; Shirude, P. S.; Rodriguez, R.; Balasubramanian, S. *Chem. Commun.* **2008**, 1467.

(38) Redman, J. E.; Granadino-Roldan, J. M.; Schouten, J. A.; Ladame, S.; Reszka, A. P.; Neidle, S.; Balasubramanian, S. *Org. Biomol. Chem.* **2009**, *7*, 76.

(39) Ladame, S.; Schouten, J. A.; Stuart, J.; Roldan, J.; Neidle, S.; Balasubramanian, S. *Org. Biomol. Chem.* **2004**, *2*, 2925.

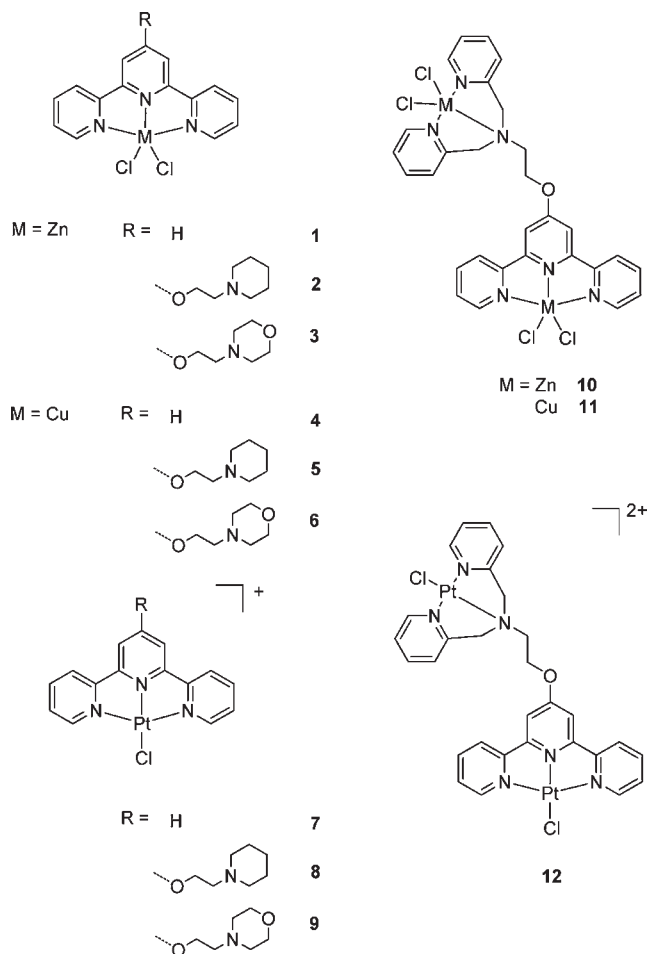
(40) Redman, J. E.; Ladame, S.; Reszka, A. P.; Neidle, S.; Balasubramanian, S. *Org. Biomol. Chem.* **2006**, *4*, 4364.

(41) Ladame, S.; Whitney, A. M.; Balasubramanian, S. *Angew. Chem., Int. Ed.* **2005**, *44*, 5736.

(42) Rao, L.; Bierbach, U. *J. Am. Chem. Soc.* **2007**, *129*, 15764.

(43) Bertrand, H.; Bombard, S.; Monchaud, D.; Teulade-Fichou, M.-P. *Nucleic Acids Symp. Ser.* **2008**, 163.

(44) Suntharalingam, K.; White, A. J. P.; Vilar, R. *Inorg. Chem.* **2009**, *48*, 9427.

**Scheme 2.** Metal Complexes Synthesised and Evaluated as DNA Binders

prepared by reacting *N,N*-bispicolyl-2-ethanolamine with 4-chloro terpyridine in the presence of KOH (Scheme 1). The reactants were stirred in degassed dimethyl sulfoxide (DMSO) at 60 °C for 4 h before being extracted into dichloromethane. After several aqueous washings, the solvent was removed to yield a brown solid. The  $^1\text{H}$  and  $^{13}\text{C}$  NMR spectra of this product provided clear evidence for the formation of  $\text{L}^3$ . The  $^1\text{H}$  NMR spectrum showed all the required signals with the correct integrals and multiplicities. The presence of nine different peaks (of equal integration) in the aromatic region is consistent with the successful attachment of the dipicolyl side arm to the terpyridine core. This was supported by the absence of the broad hydroxyl singlet associated to the starting material, *N,N*-bispicolyl-2-ethanolamine, as well as the downfield shift of the triplet associated to the  $-\text{OCH}_2-$  protons (from 3.70 ppm to 4.40 ppm) relative to the starting material. This downfield shift was also observed for the terminal methylene carbon in the  $^{13}\text{C}$  NMR spectrum.

With these three terpyridine ligands (plus unsubstituted terpyridine), 12 metal complexes with  $\text{Cu}^{\text{II}}$ ,  $\text{Pt}^{\text{II}}$ , and  $\text{Zn}^{\text{II}}$  were prepared (Scheme 2). The unsubstituted-terpyridine

complexes **1**, **4**, and **7** had been previously reported,<sup>45,46</sup> as were the platinum(II) complexes **8** and **9**.<sup>44</sup> The remaining complexes (**2**, **3**, **5**, **6**, and **10–12**) are new. The syntheses of the monozinc(II) and monocopper(II) complexes **2**, **3**, **5**, and **6**, were carried out by adding 1 equiv of the corresponding  $\text{MCl}_2$  salt to a methanolic solution of the ligand ( $\text{L}^1$  or  $\text{L}^2$ ). A similar procedure was employed to prepare the dizinc(II) and dicopper(II) complexes **10** and **11** (adding 2 equiv of the corresponding  $\text{MCl}_2$  salt to a methanolic solution of  $\text{L}^3$ ). These six complexes were characterized by spectroscopic and analytic techniques, as well as structurally in two cases (vide infra). The diplatinum(II) complex **12** was synthesized by reaction of  $\text{K}_2\text{PtCl}_4$  and  $\text{L}^3$  in DMSO for 24 h. A yellow solid was isolated from the reaction mixture. To obtain a pure sample of complex **12**, the solid was redissolved in the minimum amount of DMSO, and excess  $\text{NaPF}_6$  (as aqueous solution) was added dropwise. This induced the exchange of counterions on the complex yielding pure  $[\text{Pt}_2(\text{L}^3)\text{Cl}_2](\text{PF}_6)_2$  as an orange solid. The complex was fully characterized by spectroscopic and analytic techniques.

Before carrying out DNA binding studies with these complexes, their stability was investigated by monitoring the UV/vis spectrum of a 30  $\mu\text{M}$  solution (in Tris 10 mM-KCl 100 mM/HCl buffer) of the corresponding compound over 8 h. Over this period of time no significant changes were detected for the complexes under study. Therefore they were deemed to be stable under the conditions used in DNA binding assays.

We have previously shown by variable temperature  $^1\text{H}$  NMR spectroscopy that, in  $d_6$ -dmsO, platinum(II) complexes **8** and **9** aggregate via  $\pi$ - $\pi$  stacking.<sup>44</sup> It was therefore of interest to analyze whether the dinuclear complex **12** would behave similarly. Thus, variable temperature  $^1\text{H}$  NMR spectroscopic studies were carried out for both the free ligand  $\text{L}^3$  and diplatinum(II) complex **12**. For the free ligand, no significant changes in the aromatic region of the  $^1\text{H}$  NMR spectrum were observed upon increasing the temperature. This indicates that the free ligand does not display important  $\pi$ - $\pi$  stacking interactions in  $d_6$ -dmsO solution, which is not surprising since the pyridine groups of the free ligand are not coplanar. In contrast, significant shifts in the resonances of the aromatic protons were observed for complex **12** upon increasing the temperature from 25 to 100 °C (see Figure 1). Interestingly, not all the aromatic protons follow the same trend. While some of them shift downfield upon increasing the temperature (see top-left plot in Figure 1) others shift in the opposite direction (see bottom-left plot in Figure 1). This suggests that only some of the aromatic protons are involved in  $\pi$ - $\pi$  stacking interactions (namely,  $\text{H}_a$ ,  $\text{H}_b$ ,  $\text{H}_e$ ,  $\text{H}_g$ , and  $\text{H}_i$ ; see 2D NMR spectra in ESI for assignments/connectivity; Supporting Information, Figures S5, S6, and S7). Interestingly, these protons are not all in the terpyridine fragment but also on the DPA group. This is in contrast to the monoplatinum terpyridine complexes (compounds **8** and **9**) which in our previous studies<sup>44</sup> were shown to be fully engaged in  $\pi$ - $\pi$  stacking interactions (i.e., all the protons on the terpyridine ligand are displaced to higher chemical shifts upon increasing the temperature). Besides the above observations consistent with  $\pi$ - $\pi$  stacking, some protons shift upfield upon increasing the temperature, suggesting that

(45) Banerjee, S. R.; Zubieta, J. *Acta Crystallogr., Sect. C: Cryst. Struct. Commun.* **2005**, *C61*, m275.

(46) Huang, W.; Qian, H. *J. Mol. Struct.* **2008**, *874*, 64.



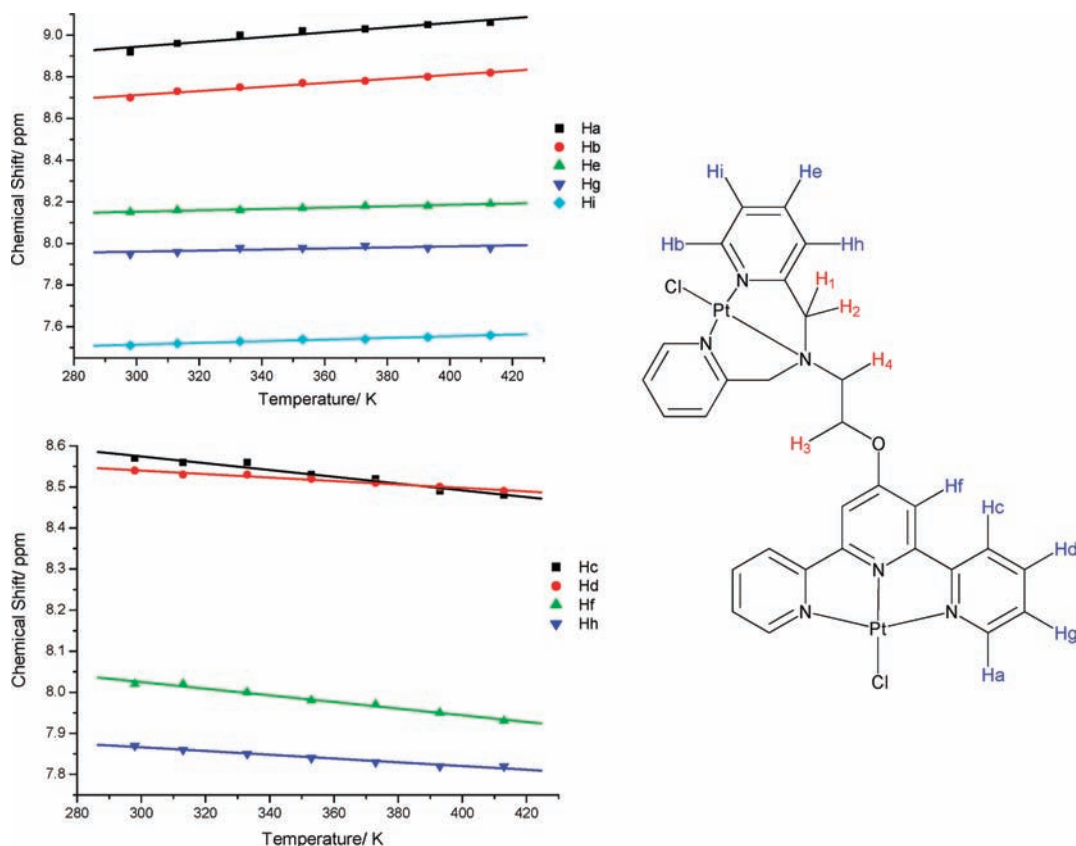


**Figure 1.** Plots showing a selection of the  $^1\text{H}$  NMR chemical shifts (of aromatic protons) versus temperature (K) for diplatinum complex **12** (8 mM). The top-left plot shows those protons that shift downfield while the bottom-left plot shows those that shift upfield.

they are not involved in  $\pi$ - $\pi$  stacking interactions but more likely in some form of hydrogen bonding that upon increasing the temperature is broken (and hence these protons become more shielded). The most likely source of this interaction is with the polar dmsol solvent; it is well established that, when dissolved in polar solvents, protons tend to shift upfield if temperature increases because of reduced solvation interactions with the solvent.

A possible explanation for these observations is that the two square planar platinum units in complex **12** interact with each other (either intra- or intermolecularly) via  $\pi$ - $\pi$  stacking interactions. Since the two platinum(II) units are different, their stacking will not be symmetric and therefore not all the protons will be affected in the same way by the aromatic ring currents associated to the shielding of protons. To gain some more insight into the nature of these interactions, a variable concentration  $^1\text{H}$  NMR experiment was carried out. Unexpectedly, practically no changes were observed when the concentration was increased from 0.5 mM to 8 mM. This suggests that the  $\pi$ - $\pi$  stacking interactions are likely to be the consequence of small aggregates (e.g., dimers of **12**) that are not modified by concentration. Another possible explanation would be that the pyridine rings of the terpyridine and DPA ligands interact intramolecularly; however, this is unlikely since the spacer between the two moieties is not flexible enough to allow them to be placed "face-to-face" in an effective manner. An X-ray crystal structure would help clarify the nature of these interactions; however, all our attempts to grow single crystals has so far failed.

**X-ray Crystal Structures of 3 and 6.** The molecular structure of **3** (Figure 2, Table 1) revealed a distorted square-based pyramidal coordination geometry at the zinc center with Cl(1) occupying the apical site position ( $\tau = 0.20$ ).<sup>47</sup> The metal lies about 0.62 Å out of the {Cl(2), N(1), N(8), N(14)} basal plane (which is only coplanar to within about 0.26 Å) toward Cl(1). The three pyridyl rings and O(19) are noticeably more distorted from planarity than in either the copper (*vide infra*) or platinum species,<sup>44</sup> with these 19 non-hydrogen atoms being coplanar to within about 0.16 Å; the metal and Cl(2) lie about 0.25 and 1.18 Å out of this plane, respectively.

The complexes pack such that ring **A** in one complex overlays ring **B** in an adjacent  $C_7$ -related complex, and *vice versa* (interaction **a** in Figure 3) with centroid $\cdots$ centroid and mean interplanar separations of about 3.61 and 3.37 Å respectively; the ring planes are inclined by about 2°. Ring **C** is approached by its counterpart in a further  $C_7$ -related complex (interaction **b** in Figure 3) with centroid $\cdots$ centroid and mean interplanar separations of about 4.03 and 3.33 Å, respectively; on account of the center of symmetry, the ring planes are perfectly parallel.

The solid state structure of the copper complex **6** (Figure 4, Table 2) showed that, like the zinc analogue, the metal has again adopted a square-based pyramidal coordination geometry with Cl(1) occupying the apical site, though it is less distorted than in the zinc species ( $\tau = 0.11$ ).<sup>47</sup> Here the copper atom lies about 0.25 Å out of the

(47) Addison, A. W.; Rao, T. N.; Reedijk, J.; Van Rijn, J.; Verschoor, G. C. *J. Chem. Soc., Dalton Trans.* **1984**, 1349.

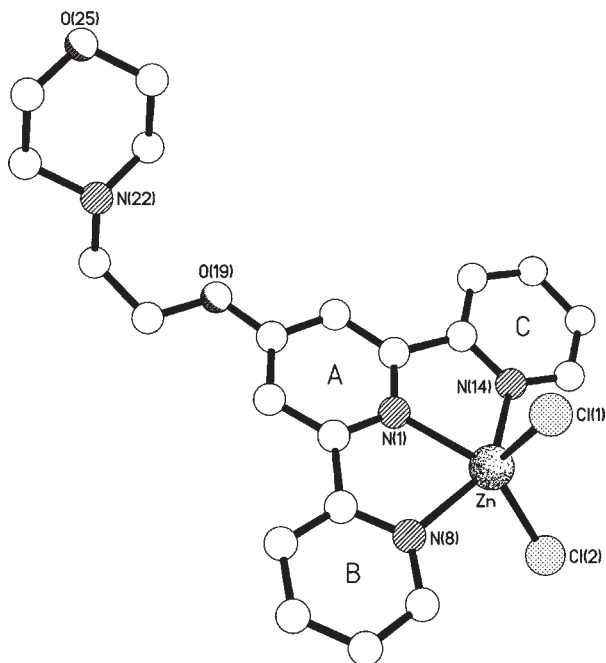


Figure 2. Molecular structure of 3.

Table 1. Selected Bond Lengths (Å) and Angles (deg) for 3

Zn–Cl(1)	2.2824(5)	Zn–Cl(2)	2.2556(5)
Zn–N(1)	2.1049(14)	Zn–N(8)	2.1953(14)
Zn–N(14)	2.2017(15)		
Cl(1)–Zn–Cl(2)	119.25(2)	Cl(1)–Zn–N(1)	105.61(4)
Cl(1)–Zn–N(8)	99.81(4)	Cl(1)–Zn–N(14)	97.78(4)
Cl(2)–Zn–N(1)	135.14(4)	Cl(2)–Zn–N(8)	96.83(4)
Cl(2)–Zn–N(14)	98.36(4)	N(1)–Zn–N(8)	74.45(5)
N(1)–Zn–N(14)	74.28(5)	N(8)–Zn–N(14)	147.22(6)

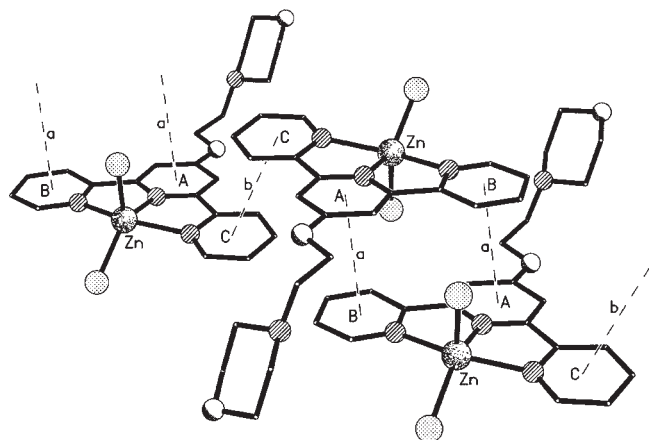


Figure 3. Part of one of the  $\pi$ - $\pi$  linked chains of complexes present in the crystals of 3. The centroid $\cdots$ centroid separations for the  $\pi$ - $\pi$  contacts (a) and (b) are about 3.61 and 4.03 Å, respectively.

{Cl(2),N(1),N(8),N(14)} basal plane (which is coplanar to within about 0.06 Å) toward Cl(1). As was seen in the previously reported platinum analogue,<sup>44</sup> the three pyridyl rings and O(19) are approximately coplanar (to within ca. 0.08 Å), though here the metal and Cl(2) lie noticeably out of this plane (by ca. 0.20 and 0.29 Å respectively). The included water molecule O(30) serves to link adjacent complexes in the *b* axis direction by hydrogen bonds to the Cl(1) chlorine atom in one molecule [O $\cdots$ Cl

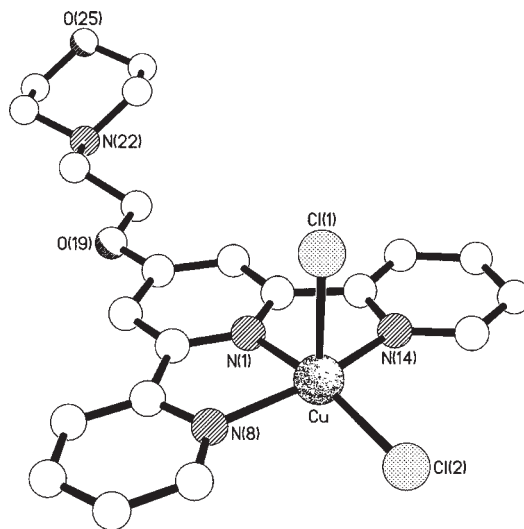


Figure 4. Molecular structure of 6.

Table 2. Selected Bond Lengths (Å) and Angles (deg) for 6

Cu–Cl(1)	2.5237(6)	Cu–Cl(2)	2.2393(5)
Cu–N(1)	1.9525(18)	Cu–N(8)	2.0526(17)
Cu–N(14)	2.0418(18)		
Cl(1)–Cu–Cl(2)	101.39(2)	Cl(1)–Cu–N(1)	94.98(6)
Cl(1)–Cu–N(8)	97.10(5)	Cl(1)–Cu–N(14)	92.59(5)
Cl(2)–Cu–N(1)	163.60(6)	Cl(2)–Cu–N(8)	99.36(5)
Cl(2)–Cu–N(14)	98.77(5)	N(1)–Cu–N(8)	79.47(6)
N(1)–Cu–N(14)	79.27(7)	N(8)–Cu–N(14)	157.30(7)

3.2006(19) Å, H $\cdots$ Cl 2.34 Å, O–H $\cdots$ Cl 161°] and the N(22) nitrogen atom in its lattice translated counterpart [O $\cdots$ N 2.986(3) Å, H $\cdots$ N 2.09 Å, O–H $\cdots$ N 173°]. The “vacant” octahedral site at the copper center is approached by the Cl(2) chlorine atom of a centrosymmetrically related complex with a Cu $\cdots$ Cl separation of about 3.46 Å; the Cl(1)–Cu $\cdots$ Cl(2A) angle is about 164°.

**Fluorescent Intercalator Displacement (FID) assay.** To evaluate the ability of these complexes to interact with different sequences of DNA, FID assays,<sup>48,49</sup> with thiazole orange (TO) as fluorophore, were carried out. Three different DNA sequences were investigated: two quadruplex forming sequences, namely, human telomeric DNA (HTelo) and *c-myc* DNA, and a 26bp duplex DNA sequence to explore the quadruplex versus duplex selectivity. The DC<sub>50</sub> values (i.e., the compound’s concentration at which TO fluorescence decreases by 50%) were determined for all the compounds, and the results are summarized in Table 3. Several interesting trends emerge from these studies: the compounds that display the highest affinity for quadruplex DNA are the dinuclear Cu–Cu and Pt–Pt complexes (**11** and **12**). Their <sup>G4</sup>DC<sub>50</sub> values are in the nM range and are comparable to previously reported quadruplex DNA binders with high binding affinities.<sup>49</sup> In addition, these two compounds display good selectivity for quadruplex versus duplex DNA (well below the threshold previously established for the FID assay<sup>49</sup>). Even in the

(48) Monchaud, D.; Allain, C.; Teulade-Fichou, M.-P. *Bioorg. Med. Chem. Lett.* **2006**, *16*, 4842.

(49) Monchaud, D.; Allain, C.; Bertrand, H.; Smargiasso, N.; Rosu, F.; Gabelica, V.; De Cian, A.; Mergny, J. L.; Teulade-Fichou, M. P. *Biochimie* **2008**, *90*, 1207.

**Table 3.**  ${}^{\text{Htelo}}\text{DC}_{50}$ ,  ${}^{\text{ds26}}\text{DC}_{50}$ , and  ${}^{\text{cmvc}}\text{DC}_{50}$  Values ( $\mu\text{M}$ ) Determined Using FID Assay for Complexes 1–12 and Ligand  $\text{L}^3$ <sup>a</sup>

compound	TO displacement			selectivity		
	${}^{\text{Htelo}}\text{DC}_{50}$ ( $\mu\text{M}$ )	${}^{\text{ds26}}\text{DC}_{50}$ ( $\mu\text{M}$ )	${}^{\text{cmvc}}\text{DC}_{50}$ ( $\mu\text{M}$ )	${}^{\text{ds26}}\text{DC}_{50}/{}^{\text{Htelo}}\text{DC}_{50}$	${}^{\text{ds26}}\text{DC}_{50}/{}^{\text{cmvc}}\text{DC}_{50}$	${}^{\text{Htelo}}\text{DC}_{50}/{}^{\text{cmvc}}\text{DC}_{50}$
$\text{L}^3$	> 2.5		> 2.5			
<b>1</b>	> 2.5		> 2.5			
<b>2</b>	> 2.5		> 2.5			
<b>3</b>	> 2.5		> 2.5			
<b>4</b>	> 2.5		> 2.5			
<b>5</b>	1.35	2.14	2.45	1.59		1.81 <sup>b</sup>
<b>6</b>	> 2.5		> 2.5			
<b>7</b>	1.46 <sup>c</sup>	> 2.5 <sup>c</sup>	0.86	2 <sup>c</sup>	2.91	1.70
<b>8</b>	1.25 <sup>d</sup>	2.44	0.26 <sup>d</sup>	1.92	9.38	4.81 <sup>d</sup>
<b>9</b>	2.24 <sup>d</sup>	> 2.5	1.01 <sup>d</sup>	2.40 <sup>e</sup>	4.72 <sup>e</sup>	2.22 <sup>d</sup>
<b>10</b>	2.25	> 2.5	1.63	1.61 <sup>e</sup>	2.87 <sup>e</sup>	1.38
<b>11</b>	0.28	1.53	0.17	6.17	9.00	1.65
<b>12</b>	0.48	> 2.5	0.26	5.81 <sup>e</sup>	10.87 <sup>e</sup>	1.77

<sup>a</sup> Values are average of three independent measurements. <sup>b</sup>  ${}^{\text{cmvc}}\text{DC}_{50}/{}^{\text{Htelo}}\text{DC}_{50}$  in these cases. <sup>c</sup>  $\text{DC}_{50}$  values obtained from *Org. Biomol. Chem.* **2007**, *5*, 2555. <sup>d</sup>  $\text{DC}_{50}$  values previously reported in *Inorg. Chem.* **2009**, *48*, 9427. <sup>e</sup> When  ${}^{\text{ds26}}\text{DC}_{50} > 2.5 \mu\text{M}$ , the selectivity is estimated using the TO displacement (%) obtained using  $2.5 \mu\text{M}$  of the ligand with ds26 and the concentration required with the respective G4 sequence to reach the same displacement,  ${}^{\text{G4C}}$ . So Selectivity =  $2.5/{}^{\text{G4C}}$ .

case of the dizinc(II) complex **10**, reasonably good  ${}^{\text{G4}}\text{DC}_{50}$  values were observed (and much lower than those for any of the monometallic zinc-terpyridine complexes). The second important observation from the data shown in Table 3 is that the monometallic complexes which display the highest affinity for quadruplex DNA are those with a square planar geometry (i.e., the  $\text{Pt}^{\text{II}}$  complexes, **7–9**). In addition, the monometallic complexes with piperidine-substituted terpyridines (e.g., the  $\text{Cu}^{\text{II}}$  complex **5** and  $\text{Pt}^{\text{II}}$  complex **8**) are considerably better quadruplex binders than their unsubstituted counterparts (or those substituted with morpholino groups).

**UV–vis DNA Binding Titrations.** UV–vis was employed to determine the binding mode and binding affinity for a selection of complexes (**8**, **11**, and **12**) toward quadruplex (HTelo) and duplex DNA (ct-DNA). The addition of quadruplex DNA to **8** (Figure 5) resulted in considerable hypochromicity of the metal perturbed intraligand  $\pi-\pi^*$  band (33%). A noticeable red shift (6 nm) was also observed. These spectral features are suggestive of an end-stacking binding mode.<sup>50</sup> The dimetallic complexes (**11** and **12**) on the other hand, displayed significantly reduced hypochromicity (15 and 18%) and very small red shifts. The latter suggest that binding may not necessarily be restricted to end-stacking and could involve supplementary interactions to DNA's loops and phosphate backbone.

In contrast, all three complexes demonstrated large hypochromicity (> 30%) upon interaction with ct-DNA; however only very small red shifts (1–2 nm) were observed. This suggests binding to ct-DNA may involve intercalation as well as other modes.

The intrinsic binding affinity toward DNA was determined by monitoring changes in complex absorption upon increasing DNA concentration. The results are summarized in Table 4. The three complexes (**8**, **11**, and **12**) were found to interact strongly to quadruplex DNA, with binding constants comparable to those of other compounds reported to be good quadruplex DNA binders ( $10^6 \text{ M}^{-1}$  range).<sup>50</sup> The mono- and dimetallic platinum(II) complexes **8** and **12** displayed reasonable selectivity (1 order

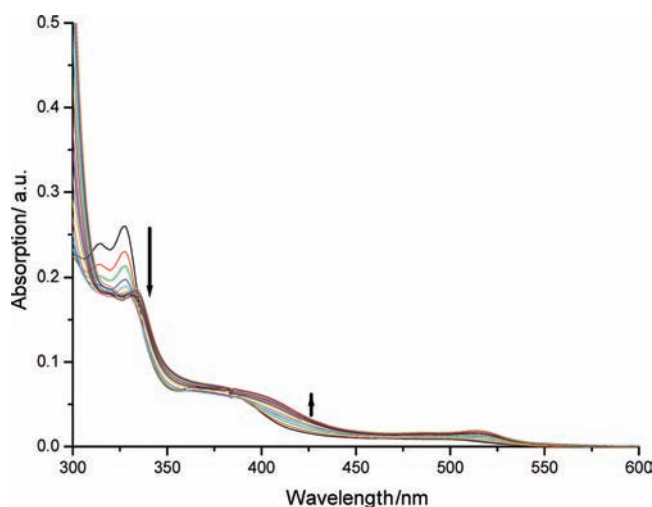


**Figure 5.** UV–vis titration of platinum complex **8** ( $20 \mu\text{M}$ ) with Htelo quadruplex DNA. The arrows indicate the change upon increasing amount of DNA added.

**Table 4.** Affinity Constants of Selected Compounds with HTelo and ct-DNA Determined by UV–vis Spectroscopy

compound	${}^{\text{HTelo}}\text{K} (\text{M}^{-1})$	${}^{\text{ct-DNA}}\text{K} (\text{M}^{-1})$	selectivity
<b>8</b> <sup>a</sup>	$1.83 \times 10^6$	$9.27 \times 10^4$	19.74
<b>11</b> <sup>b</sup>	$7.97 \times 10^6$	$6.71 \times 10^4$	118.78
<b>12</b> <sup>b</sup>	$3.28 \times 10^6$	$1.31 \times 10^5$	25.04

<sup>a</sup> Absorption measured at 328 nm (Htelo and ct-DNA). <sup>b</sup> Absorption measured at 329 nm (Htelo and ct-DNA). <sup>c</sup> Absorption measured at 334 nm (Htelo) and 328 nm (ct-DNA).

of magnitude). The dicopper complex **11** on the other hand exhibited 100-fold selectivity for quadruplex versus duplex DNA. The trend in binding affinity and selectivity determined by UV–vis across the series (**11** > **12** > **8**) is consistent with the FID data.

**Circular Dichroism (CD) Studies.** CD spectroscopy has been previously used to determine quadruplex DNA binding affinities<sup>51</sup> as well as to give some insight into

(50) Kieltyka, R.; Fakhoury, J.; Moitessier, N.; Sleiman, H. F. *Chem.–Eur. J.* **2008**, *14*, 1145.

(51) (a) Rachwal, P. A.; Fox, K. R. *Methods* **2007**, *43*, 291. (b) Ou, T. M.; Lu, Y. J.; Zhang, C.; Wang, X. D.; Tan, J. H.; Chen, Y.; Ma, D. L.; Wong, K. Y.; Tang, J. C. O.; Chan, A. S. C.; Gu, L. Q. *J. Med. Chem.* **2007**, *50*, 1465.



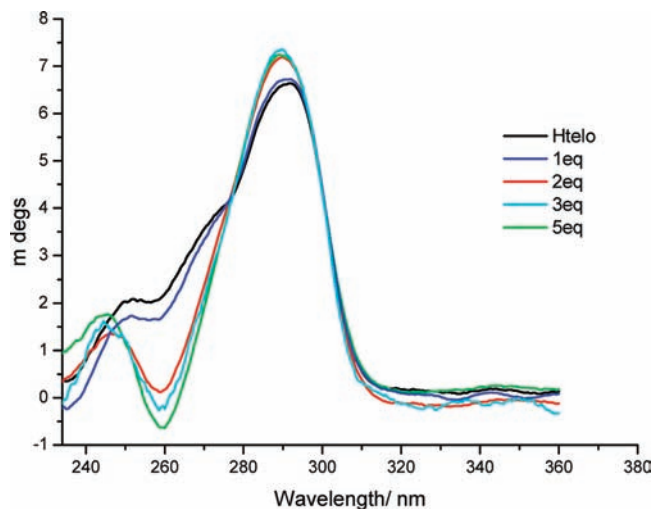


**Figure 6.** CD spectra of Htelo quadruplex DNA ( $10\ \mu\text{M}$ ) in Tris-HCl 50 mM buffer supplemented with KCl (150 mM) upon increasing addition of dicopper complex **11**.

structural changes on DNA structure upon interaction with a given compound.<sup>52,53</sup> Thus, CD spectroscopic studies were carried out to gain further insight into the interactions between the dinuclear complexes **10–12** and quadruplex DNA.

We first investigated whether these dinuclear complexes were able to induce changes on the conformation of HTelo DNA (which in the presence of potassium ions has a hybrid parallel/antiparallel structure). To this aim, increasing amounts of the corresponding complex (0.5 to 5 equiv of compound) were added to a  $10\ \mu\text{M}$  solution of HTelo quadruplex DNA in Tris-HCl/KCl buffer, and the CD spectra recorded. In the absence of any binder the CD spectrum of HTelo quadruplex DNA shows two positive maxima at about 265 and 295 nm which is indicative of a mixture of antiparallel and parallel conformations.<sup>53</sup> Upon addition of increasing amounts of each of the complexes (**10–12**) we observed a decrease in the 265 nm band and an increase of intensity of the 295 nm band (see Figure 6 for complex **11** and ESI for complexes **10** and **12**). The intensification of the 295 nm band characterizes the stabilization of the antiparallel conformation of quadruplex DNA, while the attenuation of the 265 nm band shows the destabilization of the parallel conformation. This suggests that the three dinuclear complexes, under these conditions, induce structural changes favoring the antiparallel conformation of HTelo quadruplex DNA. It should be noted, that addition of increasing amounts of  $\text{L}^3$  to HTelo DNA did not bring about any change in the CD spectrum (see Supporting Information, Figure S21 and S25) highlighting the important role played by the metal centers in binding.

It was also of interest to assess the ability of these complexes to template the formation of a quadruplex structure from an unfolded sequence. For this, 2 equiv of the corresponding compound (**10–12**) were added to a solution of HTelo DNA ( $10\ \mu\text{M}$ ) in Tris-HCl buffer (which did not contain potassium ions) and changes in

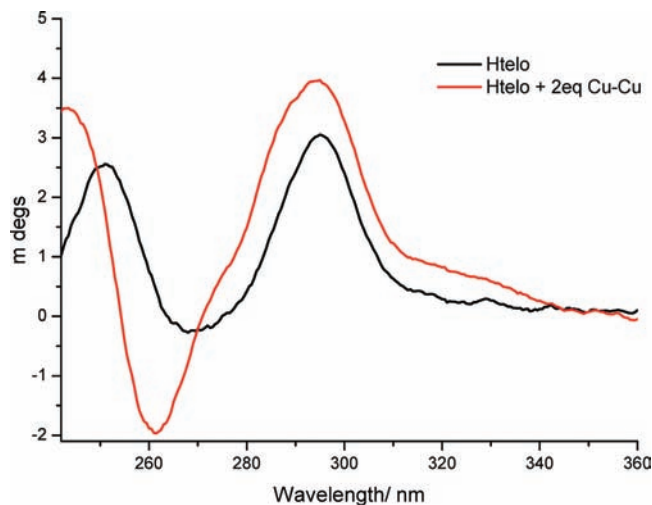


**Figure 7.** CD spectra of Htelo quadruplex DNA ( $10\ \mu\text{M}$ ) in Tris-HCl 50 mM buffer (no KCl added) with and without 2 equiv of the dicopper complex **11**.

**Table 5.** Melting Temperatures for *c-myc* Quadruplex DNA ( $5\ \mu\text{M}$ ) in the Presence of 2 Equivalents of Different Molecules

compound	$T_m$ ( $^{\circ}\text{C}$ )	$\Delta T_m^a$ ( $^{\circ}\text{C}$ )
<b>L</b> <sup>3</sup>	55.5	2.2
<b>8</b>	59.1	5.9
<b>10</b>	61.1	7.8
<b>11</b>	70.1	16.9
<b>12</b>	68.1	14.8
<b>TMPyP4</b>	64.5	11.3

<sup>a</sup>  $\Delta T_m = T_m(\text{c-myc}) - T_m(\text{c-myc} + \text{test compound})$ , where  $T_m(\text{c-myc})$  was found to be  $53.24\ ^{\circ}\text{C}$ .

the CD spectra recorded. In the absence of  $\text{K}^+$ , the CD spectrum of HTelo DNA shows two maxima: one centered at 250 nm which is associated to the unfolded sequence and one centered at 295 nm (which corresponds to some of the DNA being already folded into a quadruplex structure). Upon addition of 2 equiv of each of the complexes, we observed that the band at 250 nm disappears and the one centered at 295 nm increases (Figure 7). This indicates that even in the absence of potassium ions, the three complexes induce the formation of quadruplex DNA (largely the antiparallel conformation).

CD spectroscopy can also be used to determine the melting temperature of quadruplex DNA in the presence/absence of a given compound.<sup>51</sup> In turn, changes in the melting temperature provide a good indication of the affinity of a given compound for DNA. Thus, variable temperature CD spectra were recorded for mixtures of *c-myc* quadruplex DNA ( $5\ \mu\text{M}$ ) and the corresponding compound (2 equiv) and *c-myc*  $\Delta T_m$  values determined (see Table 5). These results confirmed the FID and UV-vis data: the dinuclear Cu–Cu and Pt–Pt complexes (**11** and **12**) display the highest affinity toward quadruplex DNA. Furthermore, the  $\Delta T_m$  values obtained for these compounds are higher than those determined for the TMPyP4 porphyrine (a compound previously reported to have high affinity for quadruplex DNA<sup>54</sup>). These studies also showed that the free ligand ( $\text{L}^3$ ) is a very poor quadruplex DNA

(52) Kypr, J.; Kejnovska, I.; Renciuik, D.; Vorlickova, M. *Nucleic Acids Res.* **2009**, *37*, 1713.

(53) Paramasivan, S.; Rujan, I.; Bolton, P. H. *Methods* **2007**, *43*, 324.

(54) Han, F. X.; Wheelhouse, R. T.; Hurley, L. H. *J. Am. Chem. Soc.* **1999**, *121*, 3561.

binder (confirming again the results obtained by FID) highlighting the importance of the metal centers in defining their binding ability.

## Conclusions

A series of mono- and dimetallic complexes with copper(II), platinum(II), and zinc(II) have been prepared, and their binding affinities toward duplex and quadruplex (HTelo and *c-myc*) DNA determined. Two important conclusions can be drawn from these results: (a) metals play a key role in defining the quadruplex DNA binding affinities of aromatic polydentate ligands (such as  $L^1$ - $L^3$ ). Upon coordination to platinum(II) or copper(II), square planar or square-based pyramidal complexes are obtained which can stack on top of the guanine quartets via  $\pi$ - $\pi$  interactions. (b) This work also shows the possibility of incorporating metals not only as a structural locus to restrict the geometry of the planar aromatic core but also as a binding element in the substituents of this core. There are very few previous studies where this idea has been explored. Therefore, we think that the current study sets the basis for a novel approach to increasing the ability of molecules to interact with and template the formation of quadruplex DNA structures.

## Experimental Details

**Materials and General Procedures.** All chemicals used in this study were purchased from Sigma-Aldrich Chemical Co. (except for  $K_2PtCl_4$  which was obtained as a loan from Johnson Matthey). The purity of the organic chemicals was verified by  $^1H$  NMR spectroscopy. *N,N*-bispicolyl-2-ethanolamine,<sup>45</sup> and complexes **1**, **4**, and **7** were prepared using previously reported procedures.<sup>45,46</sup> Ligands  $L^1$ , and  $L^2$ , and the corresponding platinum(II) complexes **8** and **9** were synthesized using the methodology we recently reported.<sup>44</sup>  $^1H$  NMR,  $^{13}C$  NMR, and  $^{31}P$  NMR spectra were recorded on a Bruker Avance 400 MHz Ultrashield NMR spectrometer.  $^1H$  COSY, NOESY and ROESY spectra were recorded on a Bruker Avance 500 MHz Ultrashield NMR spectrometer. Electrospray ionization mass spectra were recorded on Bruker Daltronics Esquire 3000 spectrometer by Mr. J. Barton (Imperial College London). Elemental analyses of the compounds prepared were performed by Mr. A. Dickerson (University of Cambridge).

**Synthesis of 2-(2,2':6',2''-terpyridine-4'-yloxy)ethyl-*N,N*-(2-pyridylmethyl)amine ( $L^3$ ).** *N,N*-bispicolyl-2-ethanolamine (250 mg, 1.0 mmol) and 4'-chloro-2,2':6',2''-terpyridine (250 mg, 0.9 mmol) were slowly added to a stirred suspension of powdered KOH (262 mg, 5.0 mmol) in DMSO (5 mL). The solution was stirred under nitrogen at 60 °C for 4 h. The reaction mixture was extracted with  $CH_2Cl_2$  (40 mL  $\times$  3), washed thoroughly with water (30 mL  $\times$  3) and dried over sodium sulfate. The solvent was removed under reduced pressure to yield the product as a brown sticky solid (256 mg, 58%);  $^1H$  NMR (400 MHz, DMSO- $d_6$ ):  $\delta_H$  8.73 (d, 2H,  $^3J_{HH}$  8.0, tpy 2-H), 8.61 (d, 2H,  $^3J_{HH}$  8.0, tpy 5-H), 8.48 (dd, 2H,  $^3J_{HH}$  8.0,  $^4J_{HH}$  2.0, py 2-H), 8.01 (dt, 2H,  $^3J_{HH}$  8.0,  $^3J_{HH}$  8.0,  $^4J_{HH}$  2.0, tpy 4-H), 7.94 (s, 2H, tpy' 3-H and 5-H), 7.73 (dt, 2H,  $^3J_{HH}$  8.0,  $^3J_{HH}$  8.0,  $^4J_{HH}$  2.0, py 4-H), 7.60 (d, 2H,  $^3J_{HH}$  8.0, py 5-H), 7.51 (ddd, 2H,  $^3J_{HH}$  8.0,  $^3J_{HH}$  8.0, tpy 3-H), 7.22 (ddd, 2H,  $^3J_{HH}$  8.0,  $^3J_{HH}$  8.0, py 3-H), 4.40 (t, 2H,  $^3J_{HH}$  6.0, ethyl 1-H), 3.92 (s, 4H, py 6-H), 3.02 (t, 2H,  $^3J_{HH}$  6.0, ethyl 2-H);  $^{13}C$  NMR (400 MHz, DMSO- $d_6$ ):  $\delta_C$  167.02, 159.78, 157.10, 155.33, 149.71, 149.21, 137.83, 136.94, 124.97, 123.07, 122.57, 121.36, 107.27, 66.70, 60.54, 52.69; ESI-MS Calcd. for  $C_{24}H_{26}N_6O$  ( $M^+$ ): 474.2 amu Found ( $M+H^+$ ): 475.0 a.m.u.; Anal. Calcd. for  $C_{24}H_{26}N_6O \cdot 1.6H_2O$ : C 69.16, H 5.85, N 16.70 Found: C 69.74, H 5.62, N 15.96.

**Synthesis of 2.** Ligand  $L^1$  (176 mg, 0.49 mmol) and  $ZnCl_2$  (67 mg, 0.49 mmol) were dissolved separately in MeOH (2.5 mL each). The methanolic solutions were combined slowly and

stirred at room temperature for 24 h. The resultant white precipitate was filtered and washed with warm MeOH and diethyl ether to yield a white crystalline solid (185 mg, 77%);  $^1H$  NMR (400 MHz, DMSO- $d_6$ ):  $\delta_H$  8.81 (br d, 2H,  $^3J_{HH}$  4.0, tpy 2-H), 8.79 (br d, 2H,  $^3J_{HH}$  8.0, tpy 5-H), 8.39 (br s, 2H, tpy' 3-H and 5-H), 8.32 (br t, 2H,  $^3J_{HH}$  6.0, tpy 4-H), 7.86 (br t, 2H,  $^3J_{HH}$  6.0, tpy 3-H), 4.56 (t,  $^3J_{HH}$  6.0, 2H, ethyl 1-H), 2.81 (t, 2H,  $^3J_{HH}$  6.0, ethyl 2-H), 2.51 (m, 4H, piperidine 2-H), 1.52 (m, 4H, piperidine 1-H), 1.43 (m, 4H, piperidine 3-H); ESI-MS Calcd. for  $C_{22}H_{24}Cl_2N_4OZn$  ( $M^+$ ): 496.0 amu Found ( $M-Cl^+$ ): 459.0 a.m.u.; Anal. Calcd. for  $C_{22}H_{24}Cl_2N_4OZn \cdot 1.7H_2O$ : C 50.10, H 5.24, N 10.62 Found: C 49.78, H 4.75, N 10.50.

**Synthesis of 3.** Ligand  $L^2$  (90 mg, 0.3 mmol) and  $ZnCl_2$  (34 mg, 0.3 mmol) were dissolved separately in MeOH (2.5 mL each). The methanolic solutions were combined slowly and stirred at room temperature for 24 h. The resultant white precipitate was filtered and washed with warm MeOH and diethyl ether to yield a white crystalline solid (120 mg, 84%);  $^1H$  NMR (400 MHz, DMSO- $d_6$ ):  $\delta_H$  8.82 (br d, 2H,  $^3J_{HH}$  4.0, tpy 2-H), 8.78 (br d, 2H,  $^3J_{HH}$  8.0, tpy 5-H), 8.39 (br s, 2H, tpy' 3-H and 5-H), 8.31 (br t, 2H,  $^3J_{HH}$  8.0, tpy 4-H), 7.86 (br t, 2H,  $^3J_{HH}$  8.0, tpy 3-H), 4.58 (t,  $^3J_{HH}$  6.0, 2H, ethyl 1-H), 3.62 (m, 4H, morpholine 1-H), 2.85 (t, 2H,  $^3J_{HH}$  6.0, ethyl 2-H), 2.51 (m, 4H, morpholine 2-H); ESI-MS Calcd. for  $C_{21}H_{22}N_4O_2Cl_2Zn$  ( $M^+$ ): 498.7 amu Found ( $M-Cl^+$ ): 463.0 a.m.u.; Anal. Calcd. For  $C_{21}H_{22}N_4O_2Cl_2Zn$ : C 50.57, H 4.45, N 11.23 Found: C 50.20, H 4.40, N 10.83.

**Synthesis of 5.** Ligand  $L^1$  (199 mg, 0.55 mmol) and  $CuCl_2 \cdot 2H_2O$  (94 mg, 0.55 mmol) were dissolved separately in MeOH (2.5 mL each). The methanolic solutions were combined slowly and stirred at room temperature for 24 h. The resultant green precipitate was filtered and washed with warm MeOH and diethyl ether. The product was purified by slow diffusion of acetone into a concentrated aqueous solution. The complex was isolated as blue crystals (180 mg, 66%); ESI-MS Calcd. for  $C_{22}H_{24}Cl_2CuN_4O$  ( $M^+$ ): 495.0 amu Found ( $M-Cl^+$ ): 458.0 a.m.u.; Anal. Calcd. For  $C_{22}H_{24}N_4OCl_2Cu \cdot 3H_2O \cdot HCl$ : C 45.14, H 5.34, N 9.57 Found: C 44.92, H 4.78, N 9.24.

**Synthesis of 6.** Ligand  $L^2$  (73 mg, 0.2 mmol) and  $CuCl_2 \cdot 2H_2O$  (34 mg, 0.2 mmol) were dissolved separately in MeOH (2.5 mL each). The methanolic solutions were combined slowly and stirred at room temperature for 24 h. The resultant green precipitate was filtered and washed with warm MeOH and diethyl ether. The product was purified by slow diffusion of acetone into a concentrated aqueous solution. The complex was isolated as blue crystals (92 mg, 88%); ESI-MS Calcd. for  $C_{21}H_{22}N_4O_2Cl_2Cu$  ( $M^+$ ): 496.9 amu Found ( $M-Cl^+$ ): 460.0 a.m.u.; Anal. Calcd. For  $C_{21}H_{22}N_4O_2Cl_2Cu \cdot H_2O$ : C 48.99, H 4.70, N 10.88 Found: C 48.84, H 4.60, N 10.68.

**Synthesis of 10.** Ligand  $L^3$  (100 mg, 0.2 mmol) and  $ZnCl_2$  (63 mg, 0.5 mmol) were dissolved separately in MeOH (2.5 mL each). The methanolic solutions were combined slowly and stirred at room temperature for 24 h. The resultant white precipitate was filtered and washed with warm MeOH and diethyl ether. The bimetallic complex was isolated as a white powder (131 mg, 81%);  $^1H$  NMR (400 MHz, DMSO- $d_6$ ):  $\delta_H$  8.93 (br s, 2H, tpy 2-H), 8.83 (d, 2H,  $^3J_{HH}$  4.0, py 2-H), 8.70 (d, 2H,  $^3J_{HH}$  8.0, py 5-H), 8.34 (t, 2H,  $^3J_{HH}$  8.0, py 4-H), 8.26 (s, 2H, tpy' 3-H and 5-H), 8.07 (br s, 2H, tpy 4-H), 7.88 (ddd, 2H,  $^3J_{HH}$  8.0,  $^3J_{HH}$  4.0, py 3-H), 7.60 (d, 2H,  $^3J_{HH}$  4.0, tpy 5-H), 7.59 (br s, 2H, tpy 3-H), 4.54 (br s, 2H, ethyl 1-H), 4.37 (br s, 4H, py 6-H), 3.12 (br s, 2H, ethyl 2-H); ESI-MS Calcd.  $C_{29}H_{26}Cl_4N_6OZn_2$  ( $M^+$ ): 745.9 amu Found ( $M-2Cl^+$ ): 673.0 a.m.u.; Anal. Calcd. For  $C_{29}H_{26}Cl_4N_6OZn_2 \cdot 2H_2O$ : C 44.47, H 3.86, N 10.73 Found: C 44.59, H 3.43, N 10.23.

**Synthesis of 11.** Ligand  $L^3$  (100 mg, 0.2 mmol) and  $CuCl_2 \cdot 2H_2O$  (80 mg, 0.5 mmol) were dissolved separately in MeOH (2.5 mL each). The methanolic solutions were combined slowly and stirred at room temperature for 24 h. The resultant



**Table 6.** Summary of Crystallographic Data for Compounds **3** and **6**<sup>a</sup>

data	<b>3</b>	<b>6</b>
chemical formula	C <sub>21</sub> H <sub>22</sub> Cl <sub>2</sub> N <sub>4</sub> O <sub>2</sub> Zn	C <sub>21</sub> H <sub>22</sub> Cl <sub>2</sub> CuN <sub>4</sub> O <sub>2</sub>
solvent		H <sub>2</sub> O
fw	498.70	514.88
<i>T</i> (°C)	−100	−100
space group	<i>P</i> $\bar{1}$ (no. 2)	<i>P</i> 2 <sub>1</sub> / <i>c</i> (no. 14)
<i>a</i> (Å)	9.7525(3)	16.01719(19)
<i>b</i> (Å)	10.3473(4)	14.02884(14)
<i>c</i> (Å)	11.4850(4)	9.97472(12)
$\alpha$ (deg)	78.493(3)	
$\beta$ (deg)	75.307(3)	103.0551(12)
$\gamma$ (deg)	89.428(3)	
<i>V</i> (Å <sup>3</sup> )	1097.53(7)	2183.41(4)
<i>Z</i>	2	4
$\rho_{\text{calcd}}$ (g cm <sup>−3</sup> )	1.509	1.566
$\lambda$ (Å)	1.54184	1.54184
$\mu$ (mm <sup>−1</sup> )	4.004	3.931
<i>R</i> <sub>1</sub> (obs) <sup>b</sup>	0.0294	0.0354
<i>wR</i> <sub>2</sub> (all) <sup>c</sup>	0.0777	0.1045

<sup>a</sup> Oxford Diffraction Xcalibur PX Ultra diffractometer, Cu–K $\alpha$  radiation, refinement based on  $F^2$ . <sup>b</sup>  $R_1 = \sum ||F_o| - |F_c|| / \sum |F_o|$ . For observed data,  $|F_o| > 4\sigma(|F_o|)$ . <sup>c</sup>  $wR_2 = \{ \sum w(F_o^2 - F_c^2)^2 / \sum w(F_o^2)^2 \}^{1/2}$ ;  $w^{-1} = \sigma^2(F_o^2) + (aP)^2 + bP$ .

green precipitate was filtered and washed with warm MeOH and diethyl ether. The product was purified by slow diffusion of acetone into a concentrated aqueous solution. The bimetallic complex was isolated as blue crystals (120 mg, 70%); ESI-MS Calcd. C<sub>29</sub>H<sub>26</sub>Cl<sub>4</sub>Cu<sub>2</sub>N<sub>6</sub>O (M<sup>+</sup>): 741.9 amu Found (M – 2Cl<sup>+</sup>): 672.0 a.m.u.; Anal. Calcd. For C<sub>29</sub>H<sub>26</sub>Cl<sub>4</sub>Cu<sub>2</sub>N<sub>6</sub>O·4H<sub>2</sub>O: C 42.71, H 4.20, N 10.31 Found: C 42.64, H 3.76, N 9.97.

**Synthesis of 12.** Ligand **3** (100 mg, 0.2 mmol) and K<sub>2</sub>PtCl<sub>4</sub> (63 mg, 0.5 mmol) were dissolved separately in DMSO (3 mL each). The solutions were combined slowly and stirred at room temperature for 24 h. The resultant orange solution was added to acetone (20 mL) giving a yellow precipitate. This was filtered and washed with acetone and diethyl ether. The solid was dissolved in the minimum amount of DMSO, to which excess NaPF<sub>6</sub> (as an aqueous solution) was added dropwise. The resultant orange precipitate was isolated by filtration and washed repeatedly with methanol and diethyl ether. The bimetallic complex was isolated as an orange powder (131 mg, 81%); <sup>1</sup>H NMR (400 MHz, DMSO-*d*<sub>6</sub>): 8.92 (d, 2H, <sup>3</sup>J<sub>HH</sub> 4.0, tpy 2-H), 8.71 (d, 2H, <sup>3</sup>J<sub>HH</sub> 4.0, py 2-H), 8.61 (d, 2H, <sup>3</sup>J<sub>HH</sub> 4.0, tpy 5-H), 8.55 (dt, 2H, <sup>3</sup>J<sub>HH</sub> 4.0, <sup>3</sup>J<sub>HH</sub> 4.0, <sup>4</sup>J<sub>HH</sub> 1.0, tpy 4-H), 8.18 (dt, 2H, <sup>3</sup>J<sub>HH</sub> 4.0, <sup>3</sup>J<sub>HH</sub> 4.0, <sup>4</sup>J<sub>HH</sub> 1.0, py 4-H), 8.06 (s, 2H, tpy' 3-H and 5-H), 7.99 (ddd, 2H, <sup>3</sup>J<sub>HH</sub> 4.0, <sup>3</sup>J<sub>HH</sub> 4.0, tpy 3-H), 7.89 (d, 2H, <sup>3</sup>J<sub>HH</sub> 4.0, py 5-H), 7.53 (br t, 2H, <sup>3</sup>J<sub>HH</sub> 4.0, py 3-H), 5.49 (d, 2H, <sup>2</sup>J<sub>HH</sub> 14.0, py 6-H), 4.96 (d, 2H, <sup>2</sup>J<sub>HH</sub> 14.0, py 6'-H), 4.73 (br s, 2H, ethyl 1-H), 3.75 (br s, 2H, ethyl 2-H); <sup>31</sup>P NMR (400 MHz, DMSO-*d*<sub>6</sub>):  $\delta_P$  −144.20 (sept, 2P, <sup>1</sup>J<sub>PF</sub> 1756, PF<sub>6</sub>); ESI-MS Calcd. for C<sub>29</sub>H<sub>26</sub>Cl<sub>2</sub>N<sub>6</sub>OPt<sub>2</sub> (M – 2PF<sub>6</sub><sup>+</sup>): 934.0 a.m.u Found (M – 2PF<sub>6</sub>+2Na<sup>+</sup>): 980.0 a.m.u.; Anal. Calcd. For C<sub>29</sub>H<sub>26</sub>Cl<sub>2</sub>F<sub>12</sub>N<sub>6</sub>OP<sub>2</sub>Pt<sub>2</sub>: C 28.42, H 2.14, N 6.89 Found: C 28.43, H 2.12, N 6.73.

**X-ray Crystallography.** Table 6 provides a summary of the crystallographic data for compounds **3** and **6** (CCDC 773943 and 773944).

**Variable Temperature <sup>1</sup>H NMR Spectroscopic Studies.** The <sup>1</sup>H NMR spectroscopic studies were all carried out in DMSO-*d*<sub>6</sub>. The variable temperature <sup>1</sup>H NMR studies of complex **12** (8 mM) were conducted on a Bruker Avance 500 MHz Ultra-shield NMR spectrometer at 293, 313, 333, 353, 373, 393, and 413.

**Fluorescent Intercalator Displacement (FID) Assays.** The assay was carried out as previously reported in the literature.<sup>48,49</sup>

**Oligonucleotide Preparation for FID Assay.** All the oligonucleotides used were purchased from Eurogentec S.A. (U.K.).

The 22AG strand (5'-AGG-GTT-AGG-GTT-AGG-GTT-AGG-G-3') and 20AG strand (5'-GG-GAG-GGT-GGG-GAG-GGT-GGG-3') were used for the human telomeric (HTelo) and *c-myc* studies, respectively. For the duplex DNA studies a 26 base-pair complementary strand was used (5'-CAA-TCG-GAT-CGA-ATT-CGA-TCC-GAT-TG-3'). The oligonucleotides were dissolved in Milli Q water to yield a 20  $\mu$ M stock solution. This was then diluted using 10 mM potassium cacodylate (pH 7.4)/50 mM potassium chloride (60 mM K<sup>+</sup>) buffer to the appropriate concentrations. Prior to use in the FID assay, the DNA strands were annealed by heating to 95 °C for 5 min and then by cooling to room temperature overnight. **Sample Preparation:** The test compounds and thiazole orange (TO) were dissolved in DMSO to give 1 mM stock solutions. The corresponding solution was then diluted using 10 mM potassium cacodylate (pH 7.4)/50 mM potassium chloride (60 mM K<sup>+</sup>) buffer to the appropriate concentrations. **FID Assay Procedure:** The FID assay was carried out as previously reported. To a mixture of DNA sequence (0.25  $\mu$ M) and TO (0.50  $\mu$ M) in 10 mM potassium cacodylate (pH 7.4)/50 mM potassium chloride (60 mM K<sup>+</sup>) buffer an increasing amount of the corresponding molecule under study was added (0.06 to 10  $\mu$ M, which corresponds to 0.25 to 40 equiv). After an equilibration time of 3 min the emission spectrum was recorded between 510 and 750 nm with an excitation wavelength of 501 nm. This was recorded using a Varian Cary Eclipse Spectrometer. The fluorescence area was calculated using the “trapezium rule” method. The area was converted into percentage TO displacement by the following formula: % TO displacement = 100 – [(fluorescence area of sample/fluorescence area of standard) × 100]. The standard fluorescence spectrum was obtained in the absence of any molecule. % TO displacement was then plotted against each of the compound concentrations to give the respective FID curves.

**UV–vis Studies.** The UV–vis spectra were recorded on a Perkin-Elmer Lambda 25 spectrometer. To determine the binding constants of the selected complexes with Htelo and ct-DNA, the complexes (10–20  $\mu$ M) were titrated with concentrated solutions of DNA (Htelo: 2.85 mM and ct-DNA: 3.78 mM) in 50 mM Tris-HCl (pH 7.4)/100 mM KCl buffer. A 1 cm path-length quartz cuvette was used to carry out the measurements. The binding constants were obtained by fitting the data to a reciprocal plot of  $D/\Delta\epsilon_{\text{ap}}$  versus  $D$  using the following equation:<sup>55</sup>  $D/\Delta\epsilon_{\text{ap}} = D/\Delta\epsilon + 1/(\Delta\epsilon \times K)$  where the concentration of DNA is expressed in terms of base pairs (determined by measuring the absorption at 260 nm and the appropriate extinction coefficients), the apparent molar extinction coefficient  $\epsilon_a = A_{\text{observed}}/[\text{Complex}]$ ,  $\Delta\epsilon_{\text{ap}} = [\epsilon_a - \epsilon_f]$  and  $\Delta\epsilon = [\epsilon_b - \epsilon_f]$ .  $\epsilon_b$  is the extinction coefficient of the DNA bound complex, and  $\epsilon_f$  is the extinction coefficient of the free complex.

**Circular Dichroism (CD) Studies.** **Oligonucleotide Preparation for CD Studies:** All oligonucleotides used were purchased from Eurogentec S.A. (U.K.). The 22AG strand (5'-AGG-GTT-AGG-GTT-AGG-G-3') and 20AG strand (5'-GG-GAG-GGT-GGG-GAG-GGT-GGG-3') were used for the human telomeric (HTelo) and *c-myc* studies, respectively. The oligonucleotides were dissolved in Milli Q water to yield a 100  $\mu$ M stock solution. This was then diluted using 50 mM Tris-HCl (pH 7.4) or 50 mM Tris-HCl (pH 7.4)/150 mM KCl buffer to 20  $\mu$ M. Prior to use in the CD assay, the DNA solution was annealed by heating to 95 °C for 5 min and then by cooling to room temperature. **Sample Preparation:** The test compounds were dissolved in DMSO to yield a 1 mM stock solution. This was then diluted using Tris-HCl or Tris-HCl/KCl buffer to the appropriate concentrations. **CD Procedure:** The CD spectra were recorded in a strain-free 10 mm × 2 mm rectangular cell path length cuvette. The data was obtained on an Applied Photophysics Ltd. Chirascan spectrometer. The CD spectra

(55) Wolfe, A.; Shimer, G. H., Jr.; Meehan, T. *Biochemistry* **1987**, *26*, 6392.

were measured in the wavelength region of 700–180 nm with the following parameters: bandwidth, 1 nm; spectral range, 230–360 nm; step-size, 0.5 nm; time-per-point, 1.5 s. The CD spectra were collected and analyzed using the Chirascan and Chirascan Viewer softwares, respectively. The following CD spectra were recorded: (1) CD spectra for the Htelo sequence (10  $\mu\text{M}$ ) with and without the presence of the test compounds (20  $\mu\text{M}$ , 2eq.) in Tris-HCl buffer, (2) CD spectra for the Htelo sequence (10  $\mu\text{M}$ ) with varying oligonucleotide/test compound ratios (1, 2, 3, 5 and 10) in Tris-HCl/KCl buffer, and (3) variable temperature CD studies were done for the *c-myc* sequence (5  $\mu\text{M}$ ) with and without the presence of the test compound (10  $\mu\text{M}$ , 2eq.) in Tris-HCl buffer.

**Acknowledgment.** The U.K.'s Engineering and Physical Sciences Research Council (EPSRC) is thanked for a studentship to K.S. and a Leadership Fellowship to R.V. Johnson Matthey PLC is thanked for a generous loan of platinum.

**Supporting Information Available:** 2D NMR spectra (COSY, NOESY, and ROESY) and variable temperature  $^1\text{H}$  NMR spectra of compound **12**. Plots for FID, UV-vis, and CD spectroscopic studies. X-ray crystallographic data and CIF files. This material is available free of charge via the Internet at <http://pubs.acs.org>. Structures have been deposited with the Cambridge Crystallographic Data Centre (<http://www.ccdc.cam.ac.uk>); CCDC numbers: 773943 and 773944).